Molecular Pharmacology Fast Forward. Published on February 21, 2020 as DOI: 10.1124/mol.119.118042
This article has not been copyedited and formatted. The final version may differ from this version.

Title page

Structures of *Mycobacterium tuberculosis* penicillin-binding protein 3 in complex with five β-lactam antibiotics reveal mechanism of inactivation

Zuokun Lu, Han Wang, Aili Zhang, Xiang Liu, Weihong Zhou, Cheng Yang, Luke Guddat, Haitao Yang, Christopher J. Schofield, Zihe Rao

Key Laboratory of Biomarker Based Rapid-detection Technology for Food Safety of Henan Province, Xuchang University, Xuchang, Henan, China (Z. L., A. Z.); College of Life Sciences (Z. L., H. W., W. Z, Z. R.) and College of Pharmacy (X. L., C. Y.), Nankai University, Tianjin, China; School of Chemistry and Molecular Biosciences, The University of Queensland, St. Lucia, QLD 4072, Australia (L. G.); School of Life Sciences, Tianjin University, Tianjin, China (H. Y.); University of Oxford, Chemistry Research Laboratory, OX1 3TA Oxford, United Kingdom (C. J. S.); National Laboratory of Macromolecules, Institute of Biophysics, Chinese Academy of Science, Beijing, China (Z. R.); and Laboratory of Structural Biology, School of Medicine, Tsinghua University, Beijing, China (Z. R.).

Molecular Pharmacology Fast Forward. Published on February 21, 2020 as DOI: 10.1124/mol.119.118042
This article has not been copyedited and formatted. The final version may differ from this version.

Running Title Page

a) Running title: Structures of *Mtb*PBP3 complexed with β-lactams antibiotics

b) Address correspondence to: Dr. Zihe Rao, College of Life Sciences, Nankai University, Tianjin, 30071, China. E-mail: raozh@mail.tsinghua.edu.cn

c) The number of text pages: 10

The number of tables: 0

The number of figures: 7

The number of references: 48

The number of words in the Abstract: 149

The number of words in the Introduction: 666

The number of words in the Discussion: 488

c) Abbreviations: TB, tuberculosis; PBP3, Penicillin-binding protein 3; *Mtb*, Mycobacterium tuberculosis; MDR, multidrug-resistant; XDR, extensively drug-resistant.

Molecular Pharmacology Fast Forward. Published on February 21, 2020 as DOI: 10.1124/mol.119.118042
This article has not been copyedited and formatted. The final version may differ from this version.

Abstract: Due to β-lactamase mediated resistance, β-lactam antibiotics were long considered ineffective drugs for tuberculosis (TB) treatment. However, some β-lactams, including meropenem and faropenem, are being re-evaluated in patients infected with TB. Penicillin-binding protein 3 (PBP3, or ftsI) is an essential transpeptidase in *Mycobacterium tuberculosis (Mtb)* required for cell division, thus is an important drug target. Structures of apo *Mtb*PBP3 and of complexes with five β-lactams, including meropenem and faropenem, reveal how they cause inactivation via formation of hydrolytically stable acyl-enzyme complexes. The structures reveal unique features of the antibiotic interactions, both in terms of differences in their binding to *Mtb*PBP3 and in comparison with structures of other PBPs and serine β-lactamases, including the tautomerisation status of the carbapenem derived acyl-enzyme complexes. The results suggest that rather than *hoping* PBP inhibitors developed for other infections will work against TB, work should focus on developing PBP inhibitors *specialized* for treating TB.

Significance Statement:

The structures *Mtb*PBP3, an essential protein in *Mycobacterium tuberculosis*, in complex with a number of widely used β-lactam antibiotics (e.g. meropenem, aztreonam and amoxicillin) were solved. This data provides new insights for next generation rational approaches to design TB specific β-lactam or non-lactam antibiotics. This manuscript is a seminal article in the field of anti-TB drug discovery and suitable for the broad readership.

Molecular Pharmacology Fast Forward. Published on February 21, 2020 as DOI: 10.1124/mol.119.118042
This article has not been copyedited and formatted. The final version may differ from this version.

Introduction

In 2016, it was estimated that there were >10 million new cases of human tuberculosis (Tb) resulting in 1.3 million deaths.(WHO, 2018) Thus, TB is one of the most lethal infections to afflict mankind. Furthermore, multidrug-resistant TB (MDR) and extensively drug-resistant (XDR) TB pose an increasing risk resulting in fatalities; <50% of diagnosed MDR TB patients were successfully treated in 2013, with this rate falling to 22% in XDR TB patients.(WHO, 2018) The spread of antibacterial resistance(Cantas *et al.*, 2013) coupled to side effects associated with the current multi-drug TB treatment regimes, means the need to develop new anti-TB agents is of growing importance. For this reason, a better knowledge of the mechanisms of drug resistance and discovering new targets will aid the development of new anti-TB drug. Bedaquiline, a first new drug approved in over forty years targets the ATP synthase(Kundu *et al.*, 2016). SQ109, a small molecule used for the treatment of TB under clinical phase 2b, is shown to bind the membrane transporter MmpL3 of mycobacterium.(Zhang *et al.*, 2019)

The clinical application of naturally derived β-lactams in the mid-20th century revolutionized antibacterial therapy – remarkably after 70 years they remain the most widely used and important antibiotics. However, because of the presence of the *BlaC* gene in *Mtb*, which encodes a highly active nucleophilic serine β-lactamase, many β-lactams can be readily hydrolyzed, resulting in little or no therapeutic value.(Flores *et al.*, 2005) The BlaC β-lactamase in *Mtb* is an extended spectrum β-lactamase (ESBL) with high levels of penicillinase and cephalosporinase activity, as well as weak carbapenemase activity.(Hugonnet and Blanchard, 2007) However, the potency of most β-lactam antibiotic classes can be restored by co-administration with a β-lactamase inhibitor, such as clavulanate, or by side chain modification. Recent studies have shown that the combination of the carbapenem meropenem and clavulanate not only has potent activity against the H37Rv strain of *Mtb in vitro*(Hugonnet *et al.*, 2009), but is also effective in XDR-TB patients – with six of seven patients on a salvage regimen containing meropenem-clavulanate showing a reduced burden of infection and one patient completely cured of the disease.(Payen *et al.*, 2012) Faropenem, the only clinically used

Molecular Pharmacology Fast Forward. Published on February 21, 2020 as DOI: 10.1124/mol.119.118042
This article has not been copyedited and formatted. The final version may differ from this version.

penem, has also been shown to efficiently kill *Mtb* in the absence of a β-lactamase inhibitor(Dhar *et al.*, 2015) and a phase 2 clinical trial is presently underway involving a combination of faropenem plus amoxicillin/clavulanate in patients with pulmonary tuberculosis (http://clinicaltrials.gov/ct2/show/NCT02349841).

The β-lactam antibiotics act as mechanism based inhibitors by targeting the cell wall modifying $_{DD}$-transpeptidases known as penicillin-binding proteins (PBPs); in contrast to their substrates which form acyl-enzyme complexes that are susceptible to nucleophilic attack, β-lactams react with PBPs to form long-lived acylated complexes. PBPs are responsible for the formation and integrity of the rigid mesh-like peptidoglycan layer exterior to the membrane surface. The most important mechanism of resistance to β-lactams is due to β-lactamases. Interestingly, β-lactamases likely evolved from a PBP/$_{DD}$-peptidase like ancestor; as a result the active sites of both are related, not only in terms of their use of a nucleophilic serine, but also with respect to general acid base catalysis and substrate binding elements.(Pratt, 2016)

M. tuberculosis PBP3 (*Mtb*PBP3), a $_{DD}$-transpeptidase, also known as the cell division protein ftsI, is an essential protein that localizes at the septum where it forms a ternary complex with other cell division proteins.(Dasgupta *et al.*, 2006; Mukherjee *et al.*, 2009; Plocinska *et al.*, 2014) Inhibition of *Mtb*PBP3 by β-lactam antibiotics results in the formation of filamentous cells and the inability to undertake replication(Slayden and Belisle, 2009). Work to develop new β-lactam based *Mtb*PBP3 inhibitors has been hindered by a lack of structural information. Here, we describe crystal structures of the soluble region of *Mtb*PBP3, both as the apo enzyme and in complex with five antibiotics (Figure 1) including meropenem and faropenem (Data collection and refinement statistics are in Table S1). These results advance our knowledge on the mechanisms of action of these β-lactam antibiotics and provide a platform for the direction of the design of new *Mtb*PBP3 inhibitors.

Molecular Pharmacology Fast Forward. Published on February 21, 2020 as DOI: 10.1124/mol.119.118042
This article has not been copyedited and formatted. The final version may differ from this version.

Materials and Methods

Chemicals. Meropenem (>98% pure), faropenem (>95% pure), ampicillin (>95% pure), amoxicillin (>99% pure), aztreonam (>98% pure) were purchased from TCI, Solarbio, Damas-beta, and SPC-scientific, respectively.

Cloning, expression, and purification. The gene encoding for *Mtb*PBP3 (spanning residue Gly123 to the end of ORF) was amplified by PCR from *Mycobacterium tuberculosis* H37Rv genomic DNA. The resulting PCR product was digested with *Bam*HI and *Xho*I and inserted into the pGEX-6p-1 expression vector. *E. coli* BL21(DE3) cells were transformed with the recombinant plasmid and the cells were cultured in LB broth at 37°C containing 100 mg/L ampicillin. Recombinant protein production was induced by adding isopropyl β-D-1-thiogalactopyranoside (IPTG) at a final concentration of 0.5 mM at 16°C. After incubation for a further 16 hours cells were harvested by centrifugation (15 min at 5000 rpm), then resuspended in PBS buffer. The cells were lysed by sonication for 20 min; the crude extracts were centrifuged at 18000 rpm for 40 min to remove cell debris. The supernatant was loaded onto a Glutathione Sepharose 4 Fast Flow (GE healthcare) column. After several rounds of alternate washing with PBS and PBS supplemented with 1 M NaCl, 100 μL of PreScission Protease (10 mg/mL) was added to the column. After an overnight-digestion, the protein was eluted by PBS and then concentrated and exchanged to buffer A (20 mM Tris) supplemented with 20 mM NaCl. *Mtb*PBP3 was then purified by anion exchange chromatography using Hitrap Q HP and size-exclusion chromatography (Superdex 200) in buffer A containing 150 mM NaCl.

Crystallization, data collection and structure determination. Crystals of *Mtb*PBP3 were obtained by hanging-drop vapor-diffusion at 20°C by mixing 1 μL of protein solution (9 mg/mL) and 1 μL of well solution containing 9% (*w*/*v*) PEG 3350, 5 mM $CoCl_2$, 2 mM $MgCl_2$ and 0.1 M HEPES pH 7.4. For the acyl intermediate-complex structures, each compound (ampicillin, faropenem, amoxicillin, meropenem, and aztreonam) was prepared in the crystallization solution at a concentration of 5 mM. 2 μL of this solution was added to the crystallization drop. The mixture was allowed to equilibrate for one day. Before data collection, the crystals were cryoprotected in solution consisting of the well solution containing 20% glycerol. The crystals were then mounted using a cryoloop (Hampton Research). All

Molecular Pharmacology Fast Forward. Published on February 21, 2020 as DOI: 10.1124/mol.119.118042
This article has not been copyedited and formatted. The final version may differ from this version.

data were collected using BL17U1 or BL19U1 at Shanghai Synchrotron Radiation Facility (SSRF) and processed using *XDS.*(Kabsch, 2010) Initial phases for apo *Mtb*PBP3 were solved by molecular replacement with *Phaser*(McCoy *et al.*, 2007) in *CCP4*(Winn *et al.*, 2011) using the structure of PBP3 from *Pseudomonas aeruginosa* (PDB ID: 3PBN) as a search model.

The structure of *Mtb*PBP3 was completed by several rounds of model building with *COOT*(Emsley and Cowtan, 2004; Emsley *et al.*, 2010) and refinement with *REFMAC5*(Murshudov *et al.*, 1997, 2011) in *CCP4* and *Phenix.*(Adams *et al.*, 2010; Afonine *et al.*, 2012) The geometric restraints for ampicillin and aztreonam were generated using the *Grade* Web Server (http://grade.globalphasing.org). Structure validation was carried out by *MolProbity*(Chen *et al.*, 2010) in *PHENIX.*(Adams *et al.*, 2010) Statistics of diffraction data and refinement are shown in Table S1.

Kinetics assays. The methods for the kinetics assays are described in the Supplemental information.

Molecular Pharmacology Fast Forward. Published on February 21, 2020 as DOI: 10.1124/mol.119.118042
This article has not been copyedited and formatted. The final version may differ from this version.

Results

Overall structure. To better understand how the β-lactam antibiotics interact with an essential PBP from *Mycobacterium tuberculosis* we determined a crystal structure (2.1 Å resolution) of the soluble region of *Mtb*PBP3 (PDB ID 6KGH), spanning residues D129 to T679 (Table S1). This structure reveals *Mtb*PBP3 has two domains: an N-terminal domain, and a highly ordered C-terminal transpeptidase domain (Figure 2A), however, two regions in the N-terminal domain are not visible in the electron density maps (Dashed line in Figure 2B). The function of the N-terminal domain of class B PBPs is yet to be fully understood, but it is proposed to interact with other proteins in the divisome.(Datta *et al.*, 2006; Mukherjee *et al.*, 2009; Sauvage *et al.*, 2014) The *Mtb*PBP3 transpeptidase domain comprises two subdomains, identified as α- and α/β (yellow and blue, respectively in Figure 2A). Three PBP/β-lactamase conserved motifs(Sauvage *et al.*, 2008; Sainsbury *et al.*, 2011) are present in the active site which is located at the interface between the α- and α/β subdomains. The nucleophilic S386 and K389, which is important in acid/base catalysis, are part of the signature SXXK motif, also found in β- lactamases, are located at the base of the active site interior (Figure 2C). The second conserved motif SXN (S441 and N443) is located on the side of the active site bordered by the α-domain (Figure 2C). The third conserved motif KTGT/S (K592, T593, G594 and T595) is located on the opposite active site face and belongs to the α/β domain (Figure 2C). The extended active site cleft accommodates the natural polypeptide substrates, and enables catalytic cross-linking of the peptide subunits of the peptidoglycans, and is also the target site for the β-lactam antibiotics (see below).

In the apo structure, the S386 side chain points toward the α/β subdomain and forms a hydrogen-bond with the backbone amide of T595 (2.9 Å), but this side-chain is 4.9 Å and 4.0 Å from K389NZ and K592NZ, respectively (Figure 2B). The sequence and fold of the transpeptidase domain of *Mtb*PBP3 is similar to that of *Pseudomonas aeruginosa* PBP3 (*Pa*PBP3(Han *et al.*, 2010)), with an RMS deviation of 2.78 Å over 294 Cα atoms. Interestingly, in the *Pa*PBP3 (PDB: 3PBN(Han *et al.*, 2010)) structure, the hydroxyl group of the residue corresponding to S386 points towards the α-

Molecular Pharmacology Fast Forward. Published on February 21, 2020 as DOI: 10.1124/mol.119.118042
This article has not been copyedited and formatted. The final version may differ from this version.

subdomain, forming two hydrogen bonds to the corresponding K389 and K592 with a distance of 2.8 Å and 2.7 Å, respectively. (Figure 2D). Thus, the apo structures of *Pa*PBP3 and *Mtb*PBP3 differ in this respect; the combined structures imply that induced fit involving a conformational change must occur in *Mtb*PBP3 to enable acylation, either by a polypeptide during catalysis or by a β-lactam antibiotic during inhibition. The apparent lack of nucleophilicity for apo *Mtb*PBP3 may reflect a means of achieving substrate selectivity.

***Mtb*PBP3 is covalently acylated by meropenem and faropenem.** Meropenem is a broad-spectrum β-lactam antibiotic belonging to the carbapenem subgroup. Although this group of β-lactam antibiotics mimics the natural substrate of $_{LD}$-transpeptidases, meropenem targets both the nucleophilic serine $_{DD}$-transpeptidases and the less common nucleophilic cysteine $_{LD}$-transpeptidases, which are also present in mycobacteria.(Kohler *et al.*, 1999; Triboulet *et al.*, 2011; Kumar *et al.*, 2012) Pre-steady-state kinetics analysis shows that *Mt*bPBP3 is irreversibly and fully inactivated by meropenem (Figure S1) with a maximum acylation rate of k_{inact} = 4.6 ± 0.12 min^{-1} (Figure S1). To visualize inactivation by meropenem, a crystal structure of the meropenem complex (PDB ID 6KGS) was determined at 2.3 Å resolution. The electron density for the bond between the Oγ atom of S386 and meropenem is continuous indicating the formation of a covalent ester bond (*i.e.* an acyl-enzyme complex) (Figure 3A). To make this bond, the side-chain of S386 rotates by ~110° compared with its conformation in the apo enzyme. In this orientation, the side-chains of S386 and K389 align parallel to each other (Figure 3B). The S441, N443, T593 and T595 side-chains also need to adjust their conformations to accommodate meropenem (Figure 3B), further supporting the proposal of substantial induced fit during inhibitor binding.

Critical interactions that stabilize meropenem in the active site are hydrogen bonds between: (i) the meropenem derived C6 hydroxyethyl oxygen and the side chain of N443; (ii) the meropenem derived C3 carboxylate and the side-chain of Thr593; and (iii) the N4 nitrogen of the meropenem derived pyrroline and the side chain of S441 (Figure 3B), though hydrophobic contacts distributed throughout the active site contribute to binding. By contrast, there is a lack of stabilizing contacts between the C2 pyrrolidine/proline derived ring and the enzyme. This is emphasized by the fact that the electron

Molecular Pharmacology Fast Forward. Published on February 21, 2020 as DOI: 10.1124/mol.119.118042
This article has not been copyedited and formatted. The final version may differ from this version.

density for this portion of the inhibitor is not as well resolved as the core carbapenem derived region. Importantly, neither in the meropenem derived structure, nor any of our other *Mtb*PBP3 inhibitor structures, is there evidence for C-C fragmentation of the acyl-enzyme complexed. This contrasts sharply with the nucleophilic cysteine $_{LD}$-transpeptidases, where, at least in some cases, e.g. with some carbapenems and faropenem, the initially formed acyl-enzyme complexes undergo fragmentation to give hydrolytically stable species.(Ammerman *et al.*, 2016) We have proposed that this difference is in part due to the differences in pKa of the ester versus thioester links in the serine $_{DD}$-transpeptidases and cysteine $_{LD}$-transpeptidases (Figure S2), a proposal supported by conservation of other features between the $_{DD}$-and $_{LD}$-transpeptidases.(Lohans *et al.*, 2019)

There is also a striking difference in the structures of the *Mtb*PBP3•meropenem and *Mtb*BlaC•meropenem complexes. In the *Mtb*BlaC•meropenem complex, the 2-pyrroline ring of meropenem/the initially formed acyl-enzyme complex is proposed to have undergone tautomerization, with the 2-pyrroline ring (enamine) converted to a 1-pyrroline ring (imine)(Hugonnet *et al.*, 2009). The same configuration for meropenem is also reported in a *Mtb* $_{LD}$-transpeptidase•meropenem complex structure (PDB ID 4GSU(Kim *et al.*, 2013)). However, in our *Mtb*PBP3•meropenem complex, the three atoms bonding to C2 are in a plane thus have sp^2 hybridization, i.e. enamine-imine tautomerisation is not observed after the β-lactam ring opens (Figure 4A). This difference may reflect subtle differences in the active site general acid/base machinery as manifest in differences between the apo-structures, including the distance between the nucleophilic oxygen and the Lys-398 Nε-amine. (Figure S3, S4). Based on the combined structural observations, we propose (Figure 4B) that after the β-lactam ring opens, the β-lactam ring derived nitrogen rapidly receives a proton from the hydroxyl group of S441 and the enamine tautomerisation state of the pyrroline ring is retained. It is also possible that (partial) β-lactam protonation occurs prior to ring opening.(Ammerman *et al.*, 2016) Note also that with some β-lactamases, S441 can act as a 'secondary' nucleophile, demonstrating its potential for involvement in reaction/catalysis.(Lohans *et al.*, 2019) In *Mtb*BlaC, we propose that the N atom does not receive a

Molecular Pharmacology Fast Forward. Published on February 21, 2020 as DOI: 10.1124/mol.119.118042
This article has not been copyedited and formatted. The final version may differ from this version.

proton, instead the pyrroline ring undergoes tautomerisation to give an imine, possibly via an anionic intermediate, with subsequent protonation at C2 (Figure 4C).(Page, 1984)

Faropenem is a broad-spectrum β-lactam that is active against a large number of Gram-positive and Gram-negative bacteria. The penems are similar to the carbapenems, but with the carbon of the carbapenems being substituted by a sulfur, which is a potential leaving group. Faropenem is much more metabolically stable than meropenem and is orally available. Importantly, faropenem taken alone is more efficient than the meropenem-clavulanate combination and isoniazid in killing *M. tuberculosis* either in the active or latent states.(Dhar *et al.*, 2015) To investigate the interactions between *Mtb*PBP3 and faropenem, a crystal structure of the complex (PDB ID 6KGT) was solved. The overall mode of binding by faropenem is similar to meropenem (Figure 5A). A similar set of interactions stabilizing the core lactam scaffold is observed as compared to meropenem, though in the faropenem derived complex S441 is not positioned to form any hydrogen bonds. By contrast, the core ring of meropenem is more tightly bound by *Mtb*PBP3 and the N atom hydrogen-bonds to S441Og. Moreover, the C3 carboxylate group of meropenem is wedged between S441 and T593 forming two hydrogen bonds. However, in the structure of the faropenem complex, the C3 carboxylate is oriented towards the solvent, only interacting with T593. As with the pyrrolidine ring in meropenem, the tetrahydrofuran ring of faropenem is exposed to the bulk solvent and is not stabilized by any interactions to the enzyme. Its conformation also appears to be flexible as the electron density is relatively weak in this region. Notably, despite the presence of the thioether group, which in other cases, enables fragmentation following acyl-enzyme formation(Ammerman *et al.*, 2016; Lohans *et al.*, 2019), no such fragmentation is observed in the *Mt*PBP3•faropenem complex, consistent with our proposal of efficient β-lactam N-protonation by *Mt*PBP3 (Figure 5B).

Aztreonam is fully recognized by *Mtb*PBP3. Aztreonam is a monobactam β-lactam which is selectively active against Gram-negative aerobic bacteria, but which exhibits little or no activity against Gram-positive bacteria.(Sykes *et al.*, 1982; Brogden and Heel, 1986) In general, combination therapies involving β-lactams and clavulanate produce improved anti-mycobacterial activity in patients with both susceptible and MDR tuberculosis, but aztreonam is an exception(Segura *et al.*, 1998). The

Molecular Pharmacology Fast Forward. Published on February 21, 2020 as DOI: 10.1124/mol.119.118042
This article has not been copyedited and formatted. The final version may differ from this version.

lack of effectiveness of aztreonam has previously been thought to be due to weak interactions with essential PBPs found in bacteria(Sykes *et al.*, 1982). However, our crystal structure of the *Mtb*PBP3•aztreonam complex (PDB ID 6KGU) shows the β-lactam carbonyl of aztreonam covalently bonded to the side-chain of S386 in *Mtb*PBP3, as occurs with meropenem and faropenem. In addition, as many as 13 hydrogen bonds and numerous hydrophobic interactions are formed between aztreonam and *Mtb*PBP3 (Figure 6A). The 2-aminothiazole side chain is accommodated in a large cavity that is formed by Q501, E383, Q597 and Y606 (Figure 6B); Q597 forms a hydrogen-bond (3.0 Å) to the methylproponoic acid group of aztreonam. In addition, the two methyl groups of the methylpropanoic acid group are accommodated by a hydrophobic wall formed by Y611, T595 and A424; the N-sulfonate group is tightly held in place by K592, S441, T593 and T595 (Figure 6C). Recent, work with avibactam derivatives (diazabicyclo[3.2.1]octanones)(Wang *et al.*, 2016), bicyclic boronates(Brem *et al.*, 2016), and structural studies including of non-covalent complex structure of *Pa*PBP3 with a hydrolyzed product of cefoperazone(Ren *et al.*, 2016), raise the possibility that non β-lactams could be used to inhibit PBPs. The extensive interactions of *Mtb*PBP3 with aztreonam, further imply it will be possible to design tight binding non-β-lactam inhibitors, not susceptible to β-lactamases, hence overcoming at least one mechanism of TB drug resistance.

Ampicillin and amoxicillin have a similar mode of binding to *Mtb*PBP3. Crystal structures of *Mtb*PBP3 in complex with the penicillin ampicillin (PDB ID 6KGW) and amoxicillin (PDB ID 6KGV) were determined at 2.41 Å and 2.3 Å resolution, respectively. The structures of these antibiotics are similar except that the phenyl ring of ampicillin is substituted by a phenol in amoxicillin. The C-3 carboxylate group of ampicillin is stabilized by hydrogen bonds (2.73 Å and 2.91 Å) to the side-chain hydroxyls of T593 and T595, respectively (Figure 7A). In addition, the hydrophobic C2 dimethyl groups of the thiazolidine ring are held in place by the A424, W425 and T578 sidechains. The C6 amido side chain group is held in place by hydrogen bonds with N443 and Q597 (Figure 7B).

Molecular Pharmacology Fast Forward. Published on February 21, 2020 as DOI: 10.1124/mol.119.118042
This article has not been copyedited and formatted. The final version may differ from this version.

Discussion

The combined crystal structures of apo *Mtb*PBP3 and the complexes with five β-lactams (Figure S5) provide detailed insight into their modes of action revealing both conserved features, such as ester formation, the role of the oxyanion hole formed by T595 and S386, and the conserved nature of acetamido/hydroxyethyl side chain binding elements. They also reveal unique features of the antibiotic interactions in terms of differences in binding to *Mtb*PBP3 by comparison with other PBPs and serine β-lactamases, most strikingly the tautomerisation status of the carbapenems.

The results support the need for future work on PBP inhibition for TB treatment. The carbapenem meropenem, shows high activity against *Mtb in vitro* and *in vivo.*(Hugonnet *et al.*, 2009; England *et al.*, 2012; Davies Forsman *et al.*, 2015) Notably, the *Mtb*BlaC β-lactamase possesses high levels of penicillinase and cephalosporinase activity, but relatively weak carbapenemase activity.(Hugonnet and Blanchard, 2007) In the structure of *Mtb*PBP3 in complex with meropenem, the pyrrolidine side chain meropenem is flexible and exposed to the solvent; it is thus reasonable to propose that it is not directly involved in substrate recognition. However, this moiety plays an important role in determining the spectrum of antimicrobial activity.(Moellering *et al.*, 1989; Papp-Wallace *et al.*, 2011) Indeed, carbapenems with a C2 pyrrolidine derivative (as in meropenem) exhibit broader antimicrobial activity.(Sunagawa *et al.*, 1990) In addition to *Mtb*BlaC, another mechanism of β-lactam resistance employed by *Mtb* involves its structurally complex cell envelope that is impermeable to many antibiotics.(Fisher and Mobashery, 2016) Our structural results suggest C2 derivatization would be profitable both in terms of minimizing *Mtb*BlaC catalyzed hydrolysis and in optimizing permeability and efflux properties of TB targeting carbapenems.

Aztreonam is inactive against *M. tuberculosis*, with or without clavulanic acid.(Segura *et al.*, 1998) Nevertheless, our structure shows that aztreonam is recognized by *Mtb*PBP3, via a binding mode involving multiple interactions, raising the possibility of using non-classical PBP inhibitor types, including non β-lactams(Brem *et al.*, 2016; Wang *et al.*, 2016) and, possibly, tight binding non-covalent inhibitors(Ren *et al.*, 2016) to inhibit *Mtb*PBPs. Such inhibitors warrant investigation, especially given

Molecular Pharmacology Fast Forward. Published on February 21, 2020 as DOI: 10.1124/mol.119.118042
This article has not been copyedited and formatted. The final version may differ from this version.

the problems of *Mtb*BlaC catalyzed lactam/acylating agent hydrolysis and localization of *M. tuberculosis* to macrophage cells.

In summary, we provided crystallographic and kinetic evidence for the mode of action of several clinically important β-lactam antibiotics targeting the essential penicillin-binging protein (PBP3) from *Mycobacterium tuberculosis*. We show that *Mtb*PBP3 is irreversibly and fully inactivated by meropenem and upon acylated, the side chain of the active serine rotates by ~110° to better accommodate the substrate. The overall mode of binding by faropenem is similar to meropenem and no fragmentation is observed in the *Mtb*PBP3•faropenem complex. Aztreonam is ineffective against tuberculosis but shows intact and extensive interactions with *Mtb*PBP3, further supporting the use of non-β-lactam as PBPs inhibitors. The results above suggest that rather than *hoping* existing PBP inhibitors developed for other infections will work against TB, work should be focused on developing PBP inhibitors *specialized* for TB treatment.

Molecular Pharmacology Fast Forward. Published on February 21, 2020 as DOI: 10.1124/mol.119.118042
This article has not been copyedited and formatted. The final version may differ from this version.

Acknowledgment

We thank Si Wu of the Institute of Biophysics, Chinese Academy of Science for the help of the stopped-flow experiment. We thank the staff at beamline of 17U1 and 19U1 of the SSRF (Shanghai Synchrotron Radiation Facility) for their assistance with data collection.

Molecular Pharmacology Fast Forward. Published on February 21, 2020 as DOI: 10.1124/mol.119.118042
This article has not been copyedited and formatted. The final version may differ from this version.

Author Contributions

Participated in research design: Lu, Zhang, C. Yang, H. Yang, Rao.

Conducted experiments: Lu, Wang, Zhang.

Contributed new reagents or analytic tools: Lu, Zhou, H. Yang.

Performed data analysis: Lu, Liu, Zhou, C. Yang, Guddat, C. Yang, H. Yang, Rao

Wrote or contributed to the writing of the manuscript: Lu, Guddat, Schofield, Rao

Molecular Pharmacology Fast Forward. Published on February 21, 2020 as DOI: 10.1124/mol.119.118042
This article has not been copyedited and formatted. The final version may differ from this version.

References

Adams PD, Afonine P V, Bunkóczi G, Chen VB, Davis IW, Echols N, Headd JJ, Hung L-W, Kapral GJ, Grosse-Kunstleve RW, McCoy AJ, Moriarty NW, Oeffner R, Read RJ, Richardson DC, Richardson JS, Terwilliger TC, and Zwart PH (2010) PHENIX: a comprehensive Python-based system for macromolecular structure solution. *Acta Crystallogr Sect D* **66**:213–221.

Afonine P V, Grosse-Kunstleve RW, Echols N, Headd JJ, Moriarty NW, Mustyakimov M, Terwilliger TC, Urzhumtsev A, Zwart PH, and Adams PD (2012) Towards automated crystallographic structure refinement with phenix.refine. *Acta Crystallogr Sect D Biol Crystallogr* **68**:352–367.

Ammerman NC, Ginell SL, Townsend CA, Bell DT, Zandi TA, Li S-G, Ekins S, Lamichhane G, Perryman AL, Lloyd EP, Kumar P, Freundlich JS, Kaushik A, and Mattoo R (2016) Non-classical transpeptidases yield insight into new antibacterials. *Nat Chem Biol* **13**:54–61.

Brem J, Cain R, Cahill S, McDonough MA, Clifton IJ, Jiménez-Castellanos JC, Avison MB, Spencer J, Fishwick CWG, and Schofield CJ (2016) Structural basis of metallo-β-lactamase, serine-β-lactamase and penicillin-binding protein inhibition by cyclic boronates. *Nat Commun* **7**:12406.

Brogden RN, and Heel RC (1986) Aztreonam. *Drugs* **31**:96–130.

Cantas L, Shah SQA, Cavaco LM, Manaia CM, Walsh F, Popowska M, Garelick H, Bürgmann H, and Sørum H (2013) A brief multi-disciplinary review on antimicrobial resistance in medicine and its linkage to the global environmental microbiota. *Front Microbiol* **4**:96.

Chen VB, Arendall WB, Headd JJ, Keedy DA, Immormino RM, Kapral GJ, Murray LW, Richardson JS, and Richardson DC (2010) MolProbity: all-atom structure validation for macromolecular crystallography. *Acta Crystallogr Sect D Biol Crystallogr* **66**:12–21.

Dasgupta A, Datta P, Kundu M, and Basu J (2006) The serine/threonine kinase PknB of Mycobacterium tuberculosis phosphorylates PBPA, a penicillin-binding protein required for cell division. *Microbiology* **152**:493–504.

Datta P, Dasgupta A, Singh AK, Mukherjee P, Kundu M, and Basu J (2006) Interaction between FtsW and penicillin-binding protein 3 (PBP3) directs PBP3 to mid-cell, controls cell septation and mediates the formation of a trimeric complex involving FtsZ, FtsW and PBP3 in mycobacteria. *Mol Microbiol* **62**:1655–1673.

Davies Forsman L, Giske CGG, Bruchfeld J, Schön T, Juréen P, Ängeby K, Forsman LD, Giske CGG, Bruchfeld J, Schön T, Juréen P, and Ängeby K (2015) Meropenem-clavulanate has high in vitro activity against multidrug-resistant Mycobacterium tuberculosis. *Int J Mycobacteriology* **4**, **Supplem**:80–81.

Dhar N, Dubée V, Ballell L, Cuinet G, Hugonnet J-E, Signorino-Gelo F, Barros D, Arthur M, and McKinney JD (2015) Rapid Cytolysis of Mycobacterium tuberculosis by Faropenem, an Orally Bioavailable β-Lactam Antibiotic. *Antimicrob Agents Chemother* **59**:1308–1319.

Emsley P, and Cowtan K (2004) Coot: model-building tools for molecular graphics. *Acta Crystallogr Sect D* **60**:2126–2132.

Emsley P, Lohkamp B, Scott WG, and Cowtan K (2010) Features and development of Coot. *Acta Crystallogr D Biol Crystallogr* **66**:486–501.

England K, Boshoff HIM, Arora K, Weiner D, Dayao E, Schimel D, Via LE, and Barry CE (2012) Meropenem-Clavulanic Acid Shows Activity against Mycobacterium tuberculosis In Vivo. *Antimicrob Agents Chemother* **56**:3384–3387.

Fisher JF, and Mobashery S (2016) β-Lactam Resistance Mechanisms: Gram-Positive Bacteria and Mycobacterium tuberculosis. *Cold Spring Harb Perspect Med* **6**:a025221.

Flores AR, Parsons LM, and Pavelka M. S. J (2005) Genetic analysis of the beta-lactamases of Mycobacterium tuberculosis and Mycobacterium smegmatis and susceptibility to beta-lactam antibiotics. *Microbiology* **151**:521–532.

Han S, Zaniewski RP, Marr ES, Lacey BM, Tomaras AP, Evdokimov A, Miller JR, and Shanmugasundaram V (2010) Structural basis for effectiveness of siderophore-conjugated monocarbams against clinically relevant strains of Pseudomonas aeruginosa. *Proc Natl Acad Sci* **107**:22002–22007.

Hugonnet JE, and Blanchard JS (2007) Irreversible inhibition of the Mycobacterium tuberculosis beta-lactamase by clavulanate. *Biochemistry* **46**:11998–12004.

Hugonnet JE, Tremblay LW, Boshoff HI, Barry CE, and Blanchard JS (2009) Meropenem-clavulanate is effective against extensively drug-resistant Mycobacterium tuberculosis. *Science* **323**:1215–1218.

Kabsch W (2010) XDS. *Acta Crystallogr D Biol Crystallogr* **66**:125–32.

Kim HS, Kim J, Im HN, Yoon JY, An DR, Yoon HJ, Kim JY, Min HK, Kim S-J, Lee JY, Han BW, and Suh SW (2013) Structural basis for the inhibition of Mycobacterium tuberculosis L,D-transpeptidase by meropenem, a drug effective against extensively drug-resistant strains. *Acta Crystallogr Sect D Biol Crystallogr* **69**:420–431.

Kohler J, Dorso KL, Young K, Hammond GG, Rosen H, Kropp H, and Silver LL (1999) In Vitro Activities of the Potent, Broad-Spectrum Carbapenem MK-0826 (L-749,345) against Broad-Spectrum β-Lactamase-and Extended-Spectrum β-Lactamase-Producing Klebsiella pneumoniae and Escherichia coli Clinical Isolates. *Antimicrob Agents Chemother* **43**:1170–1176.

Kumar P, Arora K, Lloyd JR, Lee IY, Nair V, Fischer E, Boshoff HIM, and Barry CE (2012) Meropenem inhibits D,D-carboxypeptidase activity in Mycobacterium tuberculosis. *Mol Microbiol* **86**:367–381.

Kundu S, Biukovic G, Grüber G, and Dick T (2016) Bedaquiline Targets the ε Subunit of Mycobacterial F-ATP Synthase. *Antimicrob Agents Chemother* **60**:6977–6979.

Lohans CT, Chan HTH, Malla TR, Kumar K, Kamps JJAG, McArdle DJB, van Groesen E, de Munnik M, Tooke CL, Spencer J, Paton RS, Brem J, and Schofield CJ (2019) Non-Hydrolytic β-Lactam Antibiotic Fragmentation by l,d-Transpeptidases and Serine β-Lactamase Cysteine Variants. *Angew Chemie - Int Ed* **58**:1990–1994.

McCoy AJ, Grosse-Kunstleve RW, Adams PD, Winn MD, Storoni LC, and Read RJ (2007) Phaser crystallographic software. *J Appl Crystallogr* **40**:658–674, International Union of Crystallography.

Moellering RCJ, Eliopoulos GM, and Sentochnik DE (1989) The carbapenems: new broad spectrum beta-lactam antibiotics. *J Antimicrob Chemother* **24 Suppl A**:1–7.

Mukherjee P, Sureka K, Datta P, Hossain T, Barik S, Das KP, Kundu M, and Basu J (2009) Novel role of Wag31 in protection of mycobacteria under oxidative stress. *Mol Microbiol* **73**:103–119.

Murshudov GN, Skubák P, Lebedev AA, Pannu NS, Steiner RA, Nicholls RA, Winn MD, Long F, and Vagin AA (2011) REFMAC5 for the refinement of macromolecular crystal structures. *Acta Crystallogr Sect D Biol Crystallogr* **67**:355–367.

Murshudov GN, Vagin AA, and Dodson EJ (1997) Refinement of Macromolecular Structures by the Maximum-Likelihood Method. *Acta Crystallogr Sect D Biol Crystallogr* **53**:240–255.

Page MI (1984) The mechanisms of reactions of .beta.-lactam antibiotics. *Acc Chem Res* **17**:144–151.

Papp-Wallace KM, Endimiani A, Taracila MA, and Bonomo RA (2011) Carbapenems: Past, present, and future. *Antimicrob Agents Chemother* **55**:4943 LP – 4960.

Payen MC, De Wit S, Martin C, Sergysels R, Muylle I, Van Laethem Y, and Clumeck N (2012) Clinical use of the meropenem-clavulanate combination for extensively drug-resistant tuberculosis. *Int J Tuberc Lung Dis* **16**:558–60.

Plocinska R, Martinez L, Gorla P, Pandeeti E, Sarva K, Blaszczyk E, Dziadek J, Madiraju M V., and Rajagopalan M (2014) Mycobacterium tuberculosis MtrB Sensor Kinase Interactions with FtsI and Wag31 Proteins Reveal a Role for MtrB Distinct from That Regulating MtrA Activities. *J Bacteriol* **196**:4120–4129.

Pratt RF (2016) β-Lactamases: Why and How. *J Med Chem* **59**:8207–8220.

Ren J, Nettleship JE, Males A, Stuart DI, and Owens RJ (2016) Crystal structures of penicillin-binding protein 3 in complexes with azlocillin and cefoperazone in both acylated and deacylated forms. *FEBS Lett* **590**:288–297.

Sainsbury S, Bird L, Rao V, Shepherd SM, Stuart DI, Hunter WN, Owens RJ, and Ren J (2011) Crystal structures of penicillin-binding protein 3 from Pseudomonas aeruginosa: comparison of native and antibiotic-bound forms. *J Mol Biol* **405**:173–84.

Sauvage E, Derouaux A, Fraipont C, Joris M, Herman R, Rocaboy M, Schloesser M, Dumas J, Kerff F, Nguyen-Distèche M, and Charlier P (2014) Crystal structure of penicillin-binding protein 3 (PBP3) from Escherichia coli. *PLoS One* **9**:e98042.

Sauvage E, Kerff FF, Terrak M, Ayala JA, and Charlier P (2008) The penicillin-binding proteins: structure and role in peptidoglycan biosynthesis. *FEMS Microbiol Rev* **32**:234–258.

Segura C, Salvadó M, Collado I, Chaves J, and Coira A (1998) Contribution of beta-lactamases to beta-lactam susceptibilities of susceptible and multidrug-resistant Mycobacterium tuberculosis clinical isolates. *Antimicrob Agents Chemother* **42**:1524–6.

Slayden RA, and Belisle JT (2009) Morphological features and signature gene response elicited by inactivation of FtsI in Mycobacterium tuberculosis. *J Antimicrob Chemother* **63**:451–457.

Sunagawa M, Matsumura H, Inoue T, Fukasawa M, and Kato M (1990) A novel carbapenem antibiotic, SM-7338 structure-activity relationships. *J Antibiot (Tokyo)* **43**:519–532.

Sykes RB, Bonner DP, Bush K, and Georgopapadakou NH (1982) Azthreonam (SQ 26,776), a synthetic monobactam specifically active against aerobic gram-negative bacteria. *Antimicrob Agents Chemother* **21**:85–92.

Triboulet S, Arthur M, Mainardi JL, Veckerle C, Dubee V, Nguekam-Moumi A, Gutmann L, Rice LB, and Hugonnet JE (2011) Inactivation kinetics of a new target of beta-lactam antibiotics. *J Biol Chem* **286**:22777–22784.

Wang DY, Abboud MI, Markoulides MS, Brem J, and Schofield CJ (2016) The road to avibactam: The first clinically useful non-β-lactam working somewhat like a β-lactam. *Future Med Chem* **8**:1063–1084.

WHO (2018) *Global tuberculosis report 2018*.

Winn MD, Ballard CC, Cowtan KD, Dodson EJ, Emsley P, Evans PR, Keegan RM, Krissinel EB, Leslie AGW, McCoy A, McNicholas SJ, Murshudov GN, Pannu NS, Potterton EA, Powell HR, Read RJ, Vagin A, and Wilson KS (2011) Overview of the CCP4 suite and current developments. *Acta Crystallogr D Biol Crystallogr* **67**:235–42.

Zhang B, Li J, Yang Xiaolin, Wu L, Zhang J, Yang Y, Zhao Y, Zhang L, Yang Xiuna, Yang Xiaobao, Cheng X, Liu Z, Jiang B, Jiang H, Guddat LW, Yang H, and Rao Z (2019) Crystal Structures of Membrane Transporter MmpL3, an Anti-TB Drug Target. *Cell* **176**:636-648.e13.

Molecular Pharmacology Fast Forward. Published on February 21, 2020 as DOI: 10.1124/mol.119.118042
This article has not been copyedited and formatted. The final version may differ from this version.

Footnotes

This work was supported by grants from the National Key Research and Development Program of China (Grant No. 15 2017YFC0840300), the Strategic Priority Research Program of the Chinese Academy of Sciences (Grant No. XDB08020200), the National Natural Science Foundation of China (Grant No. 81520108019), and the Science and Technology Planning Project of Henan Province of China No. 182102310071.

Molecular Pharmacology Fast Forward. Published on February 21, 2020 as DOI: 10.1124/mol.119.118042
This article has not been copyedited and formatted. The final version may differ from this version.

Legends for Figures

Figure 1. β-lactam antibiotics used in this study.

Figure 2. Images of the apo *Mtb*PBP3 structure (PDB ID 6KGH, Data Supplement 1). (A) The overall structure in cartoon representation with a transparent surface overlaid. The N-terminal domain is colored pink, the α- and α/β- subdomains of the C-terminal domain are in yellow and blue, respectively. (B) Schematic representation of the N-terminal domain, with the regions not visible in the structure represented by dashed lines. (C) The active site, with residues in the three conserved motifs residues shown as stick models. The hydrogen bonding network is shown as blue dashed lines. (D) Comparison of the active site of *Mtb*PBP3 with *Pseudomonas aeruginosa* PBP3 (*Pa*PBP3) (white). S386 of *Mtb*PBP3 points towards to the α subdomain and S386 of *Pa*PBP3 points to the opposite site domain (i.e. α/β subdomain). The side chain of S386 of *Mtb*PBP3 forms a hydrogen bond to T595 of the α subdomain and the S386 side chain of S386 of *Pa*PBP3 also forms two hydrogen bonds to K389 and K592 of the α/β subdomain. The α- and α/β *Mtb*PBP3 subdomains are in blue and yellow sticks, respectively. *Pa*PBP3 is shown as white.

Figure 3. *Mtb*PBP3 and interactions with meropenem (PDB ID 6KGS, Data Supplement 2). (A) Omit F_o - F_c electron density map (contoured at 3.0 σ) for the region including S386 and the binding region of meropenem. (B) The active site of the *Mtb*PBP3 acyl enzyme•meropenem complex (blue) in comparison with the apo enzyme (white).

Figure 4. Comparison of *Mtb*PBP3 with *Mtb*BlaC. (A) Comparison of structures of meropenem in the *Mtb*PBP3•meropenem (PDB ID 6KGS) and *Mtb*BlaC•meropenem complexes (PDB entry 3DWZ). (B) Proposal for the mechanism of β-lactam hydrolysis of meropenem by *Mtb*PBP3 based on the combined crystal structures. (C) Comparison of the structures of meropenem acylating *Mtb*PBP3 and *Mtb*BlaC.

Figure 5. Structure of *Mtb*PBP3 acylated by faropenem (PDB ID 6KGT, Data Supplement 3). (A) Comparison of structures of *Mtb*PBP3•meropenem (blue) and *Mtb*PBP3•faropenem (orange). (B) Reaction of faropenem with Ldt_{Mt2} and *Mtb*PBP3.

Molecular Pharmacology Fast Forward. Published on February 21, 2020 as DOI: 10.1124/mol.119.118042
This article has not been copyedited and formatted. The final version may differ from this version.

Figure 6. Structural views of the *Mtb*PBP3•aztreonam complex (PDB ID 6KGU, Data Supplement 4). (A) In addition to a covalent bond to S386A, a network of multiple interactions tightly binds aztreonam and *Mtb*PBP3. (B) Surface representation for the binding mode of the aztreonam acyl-enzyme complex in the active site of *Mtb*PBP3. The aminothiazole moiety slots into a deep pocket on the surface. Key active site residues of the apo enzyme are shown as grey sticks. The arrows represent the movement of these side chains to accommodate aztreonam. (C) Schematic of the interactions between aztreonam and *Mtb*PBP3. Hydrogen bonds are dashed lines. Hydrophobic interactions are curved dashed lines in magenta.

Figure 7. The crystal structure of the *Mtb*PBP3•amoxicillin complex (PDB ID 6KGV, Data Supplement 5). (A) Interactions of amoxicillin with *Mtb*PBP3. The F_o-F_c omit map for amoxicillin and S386 is overlaid and contoured at the 3.0 σ level. (B) The carbonyl oxygen of amoxicillin is located in the oxyanion hole formed by S386, T595.

Molecular Pharmacology Fast Forward. Published on February 21, 2020 as DOI: 10.1124/mol.119.118042
This article has not been copyedited and formatted. The final version may differ from this version.

Figures

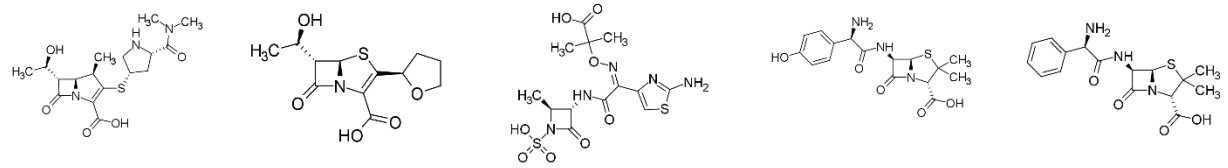

Figure 1

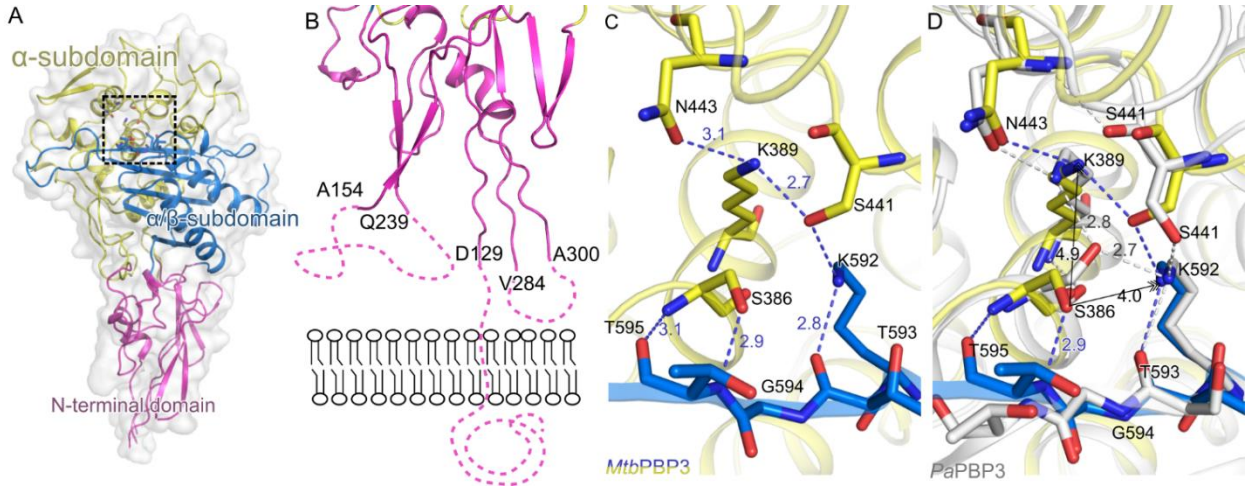

Figure 2

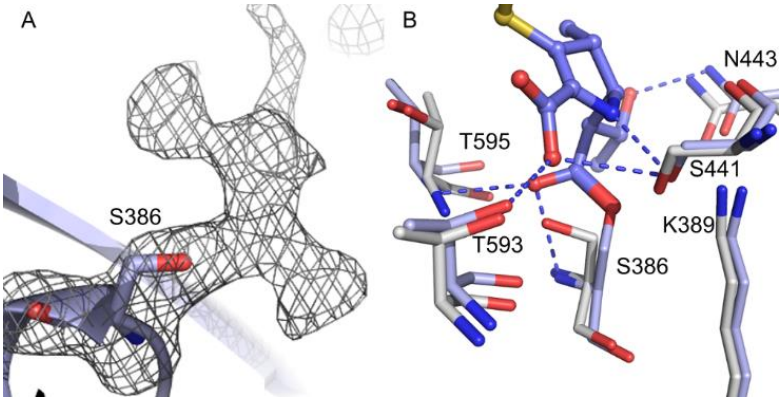

Figure 3

Molecular Pharmacology Fast Forward. Published on February 21, 2020 as DOI: 10.1124/mol.119.118042
This article has not been copyedited and formatted. The final version may differ from this version.

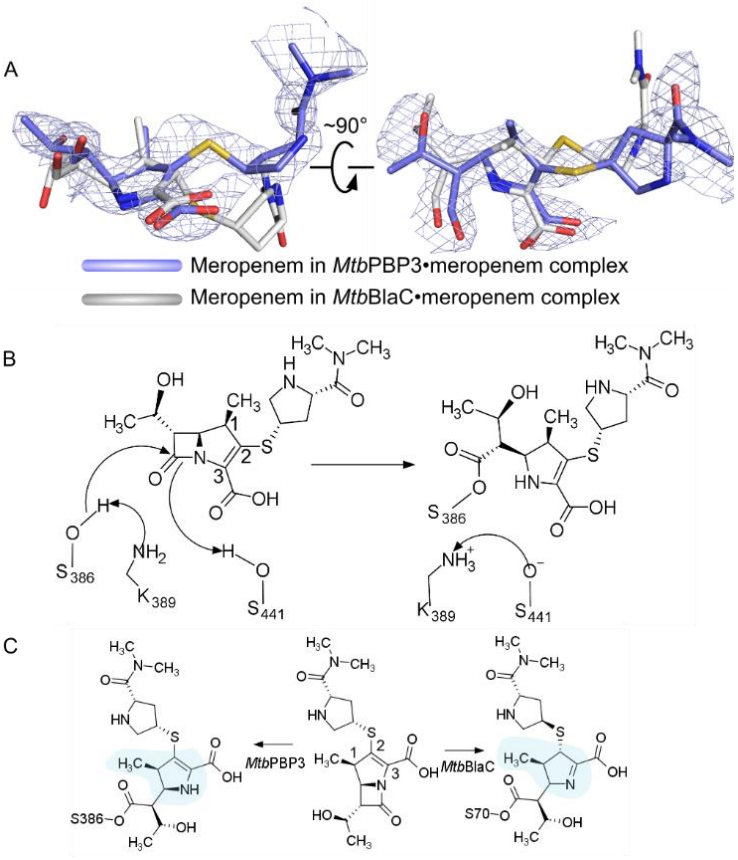

Figure 4

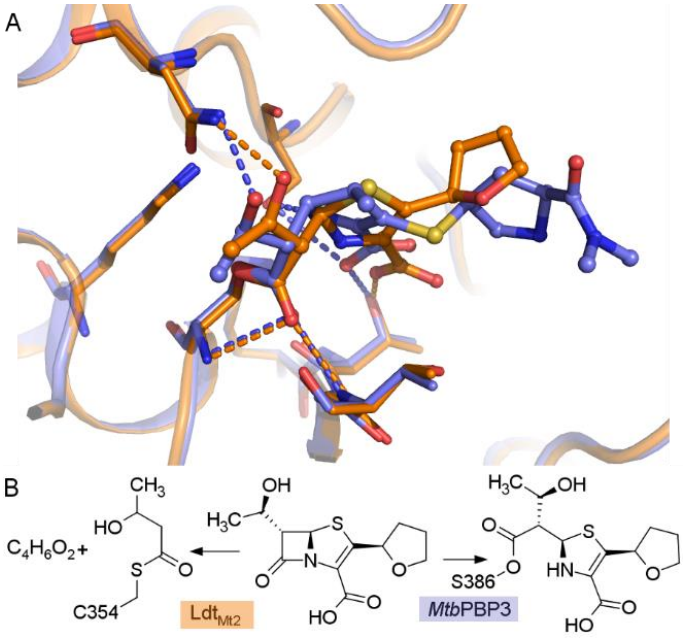

Figure 5

Molecular Pharmacology Fast Forward. Published on February 21, 2020 as DOI: 10.1124/mol.119.118042
This article has not been copyedited and formatted. The final version may differ from this version.

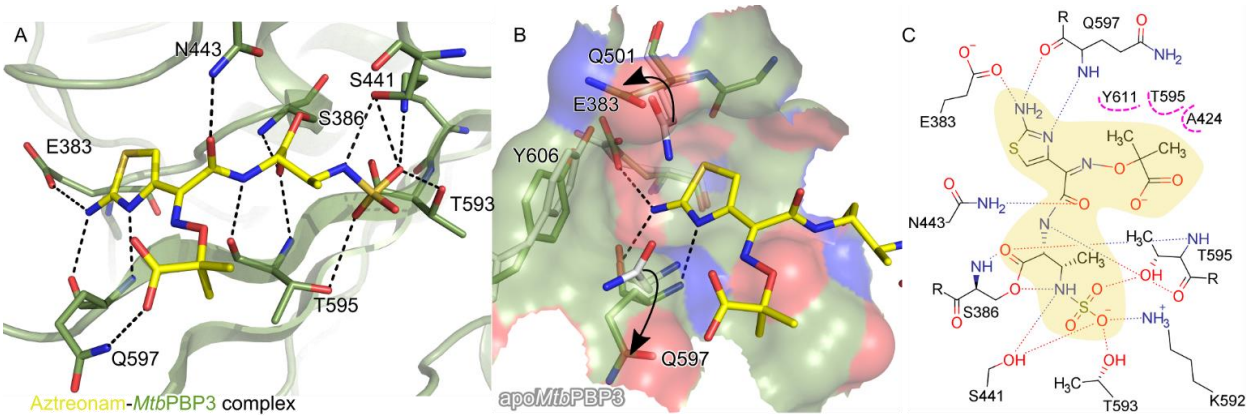

Figure 6

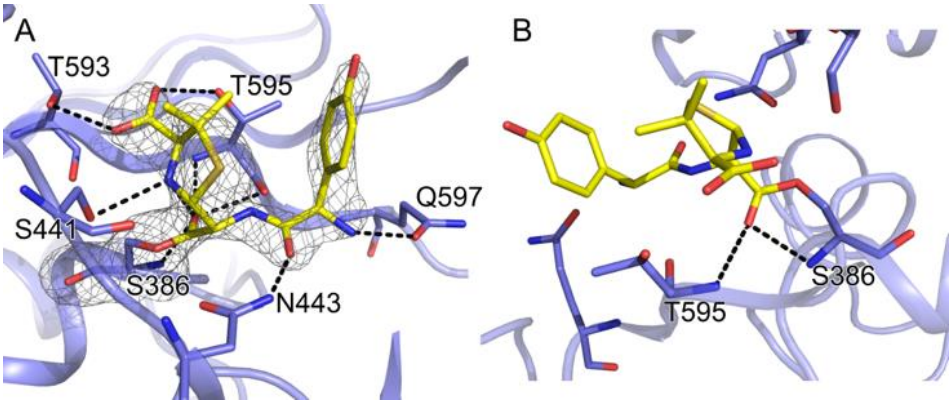

Figure 7

Supplemental Data

Molecular Pharmacology

Structures of *Mycobacterium tuberculosis* penicillin-binding protein 3 in complex with five β-lactam antibiotics reveal mechanism of inactivation

Zuokun Lu, Han Wang, Aili Zhang, Xiang Liu, Weihong Zhou, Cheng Yang, Luke Guddat, Haitao Yang, Christopher J. Schofield, Zihe Rao

Legend for supplemental information

Supplemental Figures

Figure S1. (A) Irreversible inactivation of MtbPBP3 by meropenem. MtbPBP3 at 2.25, 5.5, 8.25 M was assayed against 100 M meropenem. (B) Determination of kinact of MtbPBP3 by meropenem. 10 M MtbPBP3 was assayed against meropenem at concentrations of 25, 50, 75, 100, 150, 250, 500 M. Figures were generated by Qtiplot on Linux platform.

Figure S2. Overlaid views of MtbPBP3-faropenem (red) and LdtMt2-faropenem adduct complexes (yellow, PDB ID: 3VYP).

Figure S3. Overlaid views of apo MtbPBP3 (blue) and apo MtbBlaC (red, PDB ID: 2GDN).

Figure S4. Overlaid views of MtbPBP3-meropenem (blue) and MtbBlaC-meropenem complexes (red, PDB ID:3DWZ).

Figure S5. Chemical structures and (Fo-Fc) omit maps, contoured at 3.0 σ. Ser386 is

colored in green.

Supplemental table

Table S1. Data collection and refinement statistics for the MtbPBP3 structures.

Supplemental PDB files

Supplemental PDB files 1 - Crystal structure of Penicillin binding protein 3 (PBP3) from Mycobacterium tuberculosis, complexed with amoxicillin

Supplemental PDB files 2 - Crystal structure of Penicillin binding protein 3 (PBP3) from Mycobacterium tuberculosis, complexed with ampicillin

Supplemental PDB files 3 - Crystal structure of Penicillin binding protein 3 (PBP3) from Mycobacterium tuberculosis, complexed with meropenem

Supplemental PDB files 4 - Crystal structure of Penicillin binding protein 3 (PBP3) from Mycobacterium tuberculosis, complexed with faropenem

Supplemental PDB files 5 - Crystal structure of Penicillin binding protein 3 (PBP3) from Mycobacterium tuberculosis, complexed with aztreonam

Supplemental PDB files 6 - Crystal structure of Penicillin binding protein 3 (PBP3) from Mycobacterium tuberculosis (apo-form)

SI METHODS Kinetics assays. Rapid kinetic analyses were performed at room temperature (20°C) by measuring the decrease in absorbance at 299 nm using a stopped flow apparatus (Applied Photophysics SX20) coupled to a monochromator. The non-enzymatic rate of meropenem hydrolysis was measure for 5 min at various concentrations of meropenem (50 μM, 100 μM, and 200 μM).

Inactivation kinetics analysis were performed as previously described[1]. Briefly, *Mtb*PBP3 (16.5 mM) is incubated with different concentration of meropenem (25 mM, 50 mM, 100 mM, 250 mM, and 500 mM). Time courses of hydrolysis were first fitted to the pseudo-first order rate equation

$$[EI^*] = [E_{total}](1 - e^{-k_{obs}t})$$

where, [*EI**] is the concentration of the covalent complex; [E_{total}] is the concentration of enzyme; k_{obs} is a constant, meaning the rate of hydrolysis observed with unit of min^{-1}; *t* is time.

For determination of the catalytic constants k_{inact} and K_{app}, the values of k_{obs} obtained in the last step were plotted as a function of meropenem concentration [*I*] (Figure S1B), and regression analysis was performed using the equation

$$k_{obs} = \frac{k_{inact}[I]}{[I] + K_i}$$

in which k_{inact} is the first-order constant for acylenzyme formation, and K_i is a constant. Qtiplot was used to process the data and plot the figures. Experiments of non-enzymatic rate of meropenem hydrolysis were performed in a single replicate. Experiments of inactivation kinetics were performed in triplicate.

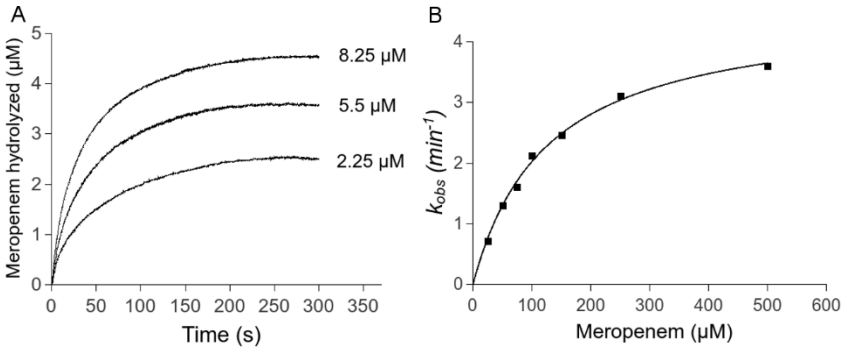

Figure S1. (A) Irreversible inactivation of *Mtb*PBP3 by meropenem. *Mtb*PBP3 at 2.25, 5.5, 8.25 μM was assayed against 100 μM meropenem. (B) Determination of k_{inact} of *Mtb*PBP3 by meropenem. 10 μM *Mtb*PBP3 was assayed against meropenem at concentrations of 25, 50, 75, 100, 150, 250, 500 μM. Figures were generated by Qtiplot on Linux platform.

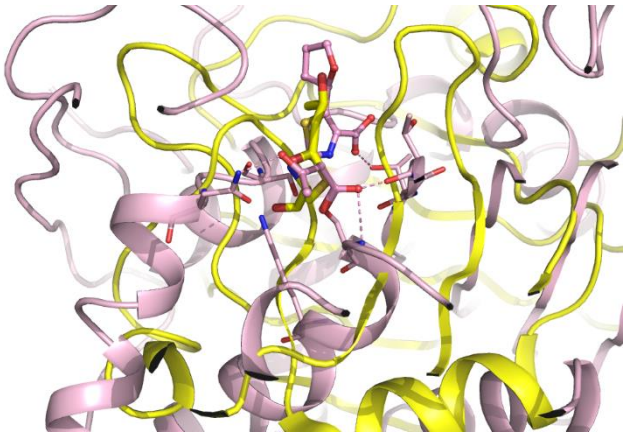

Figure S2. Overlaid views of *Mtb*PBP3-faropenem (red) and Ldt_{Mt2}-faropenem adduct complexes (yellow, PDB ID: 3VYP).

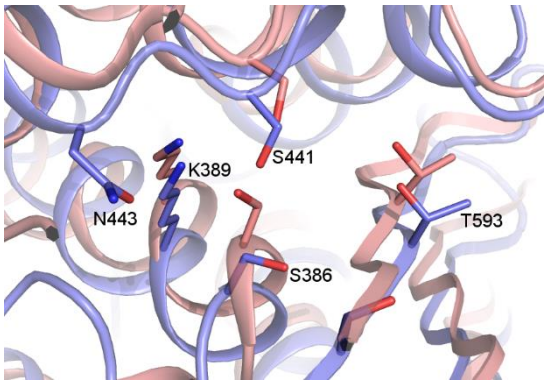

Figure S3. Overlaid views of apo *Mtb*PBP3 (blue) and apo *Mtb*BlaC (red, PDB ID: 2GDN).

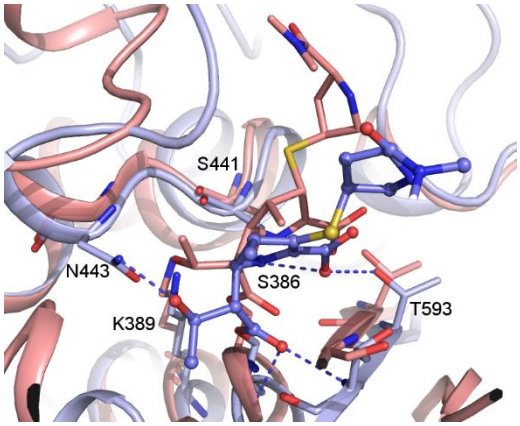

Figure S4. Overlaid views of *Mtb*PBP3-meropenem (blue) and *Mtb*BlaC-meropenem complexes (red, PDB ID:3DWZ).

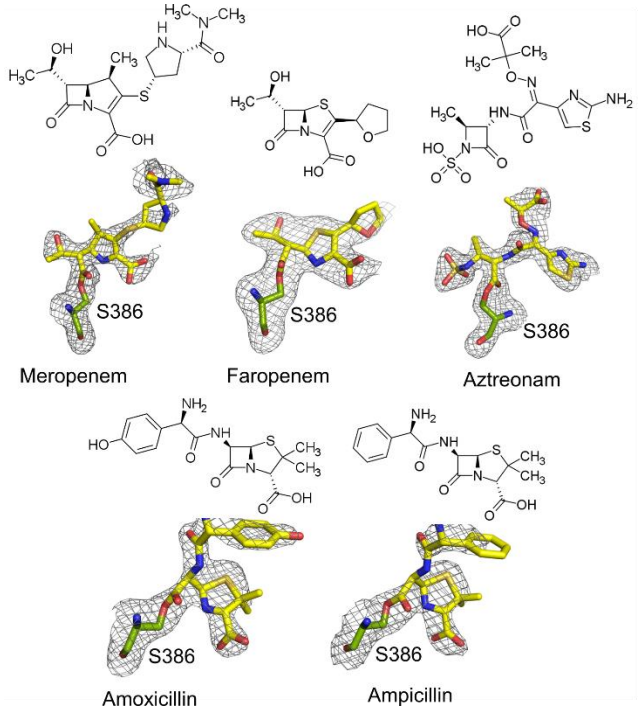

Figure S5. Chemical structures and (F_o-F_c) omit maps, contoured at 3.0 σ. Ser386 is colored in green.

Table S1. Data collection and refinement statistics for the *Mtb*PBP3 structures.

Data set	apo enzyme (PDB ID 6KGH)	meropenem complex (PDB ID 6KGS)	faropenem complex (PDB ID 6KGT)	aztreonam complex (PDB ID 6KGU)	ampicillin complex (PDB ID 6KGW)	amoxicillin complex (PDB ID 6KGV)
Data collection						
X-ray source	SSRF BL19U1	SSRF BL19U1	SSRF BL19U1	SSRF BL19U1	SSRF BL19U1	SSRF BL17U1
Wavelength (Å)	0.97776	0.978460	0.978530	0.97846	0.97846	0.97946
Space group	*C*2	*C*2	*C*2	*C*2	*C*2	*C*2
Cell parameters *a, b, c* (Å), β (°)	97.7 84.3 90.5 111.61	96.8 85.1 90.7 111.56	97.0 84.8 90.9 111.4	96.9 84.6 90.2 111.954	97.2 84.2 90.5 111.313	96.6 83.8 90.1 111.71
Resolution range (Å)	50-2.10 (2.23-2.10)	45-2.31 (2.39-2.31)	42.43-2.31 (2.39-2.31)	44.94-2.10 (2.18-2.10)	47.8-2.41 (2.49-2.41)	44.89-2.30 (2.38-2.30)
Unique reflections	39437 (3914)	30075 (2994)	30173 (2984)	38528 (3748)	26376 (2587)	29580 (2910)
Completeness (%)	99(98)	100 (99)	99 (100)	98 (97)	99 (97)	99 (99)
Redundancy	3.5 (3.3)	6.8 (6.7)	6.8 (6.8)	7.0 (7.2)	3.4 (3.3)	3.7 (3.7)
$<I/\sigma(I)>$	10.9 (2.2)	9.31 (2.65)	22.97 (3.18)	12.43 (2.82)	10.76 (1.44)	13.94 (2.01)

R_{meas} (%)	8.7 (57.2)	14.1 (58.4)	5.7 (62.6)	10.4 (60.5)	8.4 (88.8)	7.5 (78.4)
Refinement statistics						
Resolution range (Å)	48.1-2.1 (2.42-2.10)	47.63-2.31 (2.39-2.31)	42.43-2.31 (2.39-2.31)	44.94-2.11 (2.18-2.11)	47.8-2.41 (2.49-2.41)	44.89-2.30 (2.38-2.30)
R_{work}/R_{free} (%)	19.2/23.1 (22.9/27.2)	19.3/22.6 (23.1/27.4)	20.2/24.5 (25.2/30.2)	18.8/22.3 (22.3/26.6)	19.7/25.0 (30.1/36.2)	19.2/23.9 (2.51/30.1)
No. of non-H atoms	3475	3513	3489	3615	3497	3569
Protein	3319	3364	3351	3359	3361	3368
Ligand	0	26	19	28	24	25
Water	152	139	117	225	109	172
Average *B* factor ($Å^2$)	37.3	25.6	53.49	37.47	49.58	52.35
Protein	37.0	25.6	53.31	36.98	49.48	52.14
Ligand	n/a	37.7	64.96	43.9	55.2	59.8
Water	43.2	29.9	54.83	43.77	51.09	55.50
R.m.s. deviations						

Bond length (Å)	0.0079	0.0086	0.008	0.008	0.008	0.007
Bond angle (°)	0.8833	0.9748	0.97	0.87	0.91	0.87
Ramachandran plot						
Favored (%)	98.6	98.2	98.2	98.2	97.6	98.4
Outlier (%)	0	0	0.23	0	0.22	0
CC1/2	0.996(0.892)	0.991 (0.883)	0.999 (0.888)	0.996 (0.891)	0.996 (0.752)	0.998 (0.725)

SI REFERENCES

1. Triboulet, S.; Arthur, M.; Mainardi, J. L.; Veckerle, C.; Dubee, V.; Nguekam-Moumi, A.; Gutmann, L.; Rice, L. B.; Hugonnet, J. E. Inactivation Kinetics of a New Target of Beta-Lactam Antibiotics. J Biol Chem 2011, 286 (26), 22777–22784.